Received: 14 April 2021 | Revised: 30 July 2021 | Accepted: 11 August 2021

DOI: 10.1111/jnc.15492

Journal of Neurochemistry JNC The Official Journal of the International Society for Neurochemistry WILEY

ORIGINAL ARTICLE

A new brain-penetrant glucosylceramide synthase inhibitor as potential Therapeutics for Gaucher disease

Takahiro Fujii[1] | Yuta Tanaka[1] | Hideyuki Oki[2] | Sho Sato[3] | Sachio Shibata[2] | Takamitsu Maru[2] | Yuta Tanaka[4] | Maiko Tanaka[1] | Tomohiro Onishi[1]

[1]Neuroscience Drug Discovery Unit, Research, Takeda Pharmaceutical Company Limited, Fujisawa, Kanagawa, Japan

[2]Discovery Biology, Discovery Science, Axcelead Drug Discovery Partners, Inc., Fujisawa, Kanagawa, Japan

[3]Drug Metabolism and Pharmacokinetics Research Laboratories, Research, Takeda Pharmaceutical Company Limited, Fujisawa, Kanagawa, Japan

[4]Drug Discovery Sciences, Research, Takeda Pharmaceutical Company Limited, Fujisawa, Kanagawa, Japan

Correspondence
Tomohiro Onishi and Yuta Tanaka, Takeda Pharmaceutical Company Limited, 26-1, Muraoka-Higashi 2-chome, Fujisawa, Kanagawa 251-8555, Japan.
Email: tomohiro.onishi@takeda.com(T. O); yuta.tanaka@takeda.com(Y. T)

Funding information
Takeda Pharmaceutical Company

Abstract

Gaucher disease (GD), the most common lysosomal storage disorders, is caused by *GBA* gene mutations resulting in glycosphingolipids accumulations in various tissues, such as the brain. While suppressing glycosphingolipid accumulation is the central strategy for treating peripheral symptoms of GD, there is no effective treatment for the central nervous system symptoms. As glycosphingolipid biosynthesis starts from ceramide glycosylation by glucosylceramide synthase (GCS), inhibiting GCS in the brain is a promising strategy for neurological GD. Herein, we discovered T-036, a potent and brain-penetrant GCS inhibitor with a unique chemical structure and binding property. T-036 does not harbor an aliphatic amine moiety and has a noncompetitive inhibition mode to the substrates, unlike other known inhibitors. T-036 exhibited sufficient exposure and a significant reduction of glucosylsphingolipids in the plasma and brain of the GD mouse model. Therefore, T-036 could be a promising lead molecule for treating central nervous system symptoms of GD.

KEYWORDS
drug discovery, gaucher disease, glucosylceramide synthase inhibitor, glucosylsphingosine, lysosomal storage disorder

1 | INTRODUCTION

Gaucher disease (GD), one of the most prevalent lysosomal storage disorders (LSDs), is caused by mutations in the *GBA* gene which encodes glucocerebrosidase. Glycosphingolipids (GSLs) such as glucosylceramide (GlcCer) and glucosylsphingosine (GlcSph) are substrates of glucocerebrosidase, and GD is characterized by the pathological accumulation of these GSLs. Clinical features of GD include anemia, thrombocytopenia, enlargement of the liver and spleen and bone dysplasia. Additionally, there are cases showing neurological symptoms such as seizures, cognitive impairment, ataxia, and lack of coordination, categorized into GD type 2 or 3 in distinction from type 1, nonneuropathic GD (Alaei et al., 2019). GlcSph in plasma increases and is considered a biomarker for GD progression (Dekker et al., 2011; Rolfs et al., 2013). The level of GlcSph in the brain is elevated in GD type 2 and 3 patients but not in type 1 (Nilsson & Svennerholm, 1982; Orvisky et al., 2002). Therefore, GlcSph accumulation in the brain could be a key driver of the pathogenesis of neuropathic GD. In fact, the neurotoxic effect of GlcSph, such as induced apoptosis, has been reported in in vitro studies (Schueler et al., 2003; Sueyoshi et al., 2001).

Therapeutic approaches, such as enzyme replacement therapy using recombinant glucocerebrosidase and substrate reduction therapy using miglustat (Cox et al., 2003) or eliglustat (Smid &

Abbreviations: AS-MS, affinity selection mass spectrometry; CNS, central nervous system; GCS, glucosylceramide synthase; GD, gaucher disease; GlcCer, glucosylceramide; GlcSph, glucosylsphingosine; GSLs, glycosphingolipids; LSD, lysosomal storage disorder; PD, pharmacodynamics; PK, pharmacokinetics.

Hollak, 2014), have been approved for the treatment of GD. While these therapies address peripheral symptoms of GD, neither addresses the symptoms in the central nervous system (CNS) (Weiss et al., 2015). Recombinant glucocerebrosidase and eliglustat have difficulty crossing the blood–brain barrier because of its considerable molecular weight and efflux by MDR1, respectively (Larsen et al., 2012; Shayman, 2010). Although miglustat crosses the blood-brain barrier to some extent in the preclinical study (Treiber et al., 2007), it is reportedly ineffective in neuropathic GD in a clinical trial (Schiffmann et al., 2008), possibly due to its lack of pharmacological potency to achieve effective brain exposure.

Both eliglustat and miglustat inhibit GlcCer synthase (GCS), which form GlcCer from UDP-glucose and ceramide. GlcCer is converted to GlcSph via deacylation (van Eijk et al., 2020; Revel-Vilk et al., 2020). Miglustat's inhibitory potency of GCS, at the IC_{50} value of 5–50 μM, was not strong (Smid et al., 2016). Therefore, a GCS inhibitor with superior brain penetration and stronger potency would suppress brain GlcSph accumulation and offer treatment for neuropathic GD. This hypothesis is supported by the recently discovered brain-penetrant GCS inhibitors, venglustat and GZ667161, which demonstrate therapeutic potential with their reduction of GSLs in several LSD mouse models (Ashe et al., 2015; Cabrera-Salazar et al., 2012; Marshall et al., 2016, 2019; Sardi et al., 2017).

However, since GCS is a transmembrane protein, it is hard to purify. Therefore, its structural information is difficult to obtain, and its mechanism yet to be fully delineated. As a result, it is challenging to create a potent GCS inhibitor via rational design. Miglustat and eliglustat were discovered based on chemical structures mimicking substrates of GCS (Abe et al., 1995; Gu et al., 2017) and harbor an aliphatic amine moiety. While the aliphatic amine plays a role to enhance inhibitory activity against GCS (Abe et al., 1995; Alaei et al., 2019), it could potentially increase the risk of side effects through interaction with off-targets such as glucosyl transferases, glycosidases, or other molecules (McEachern et al., 2007; Wennekes et al., 2010).

Herein, we constructed a high-throughput screening system to discover a novel, potent GCS inhibitor, identified as T-036, with a chemical structure distinct from an aliphatic amine moiety. We profiled T-036 by examining its binding to GCS, assessing substrate competition, and comparing it to the known GCS inhibitors, such as eliglustat and venglustat. Also, an in vivo PK/PD study was conducted to evaluate the therapeutic potential of T-036 for GD treatment.

2 | MATERIALS AND METHODS

2.1 | Materials availability

Key resources and catalog numbers are listed in Table S1. Further information and requests for resources and reagents should be directed to and fulfilled by the Lead Contact, Tomohiro Onishi (tomohiro.onishi@takeda.com).

2.2 | Animals

Male C57BL/6J mice (6 weeks old) were purchased from CLEA Japan Inc., and male Gba D409V knock-in (KI) mice (C57BL/6N-Gba<tm1.1Mjff>/J) were purchased from the Jackson laboratory and were bred. They were housed in groups and kept on a 12-h light/dark cycle and provided ad libitum access to food and water. After acclimation for at least 1 week, animals were used in experiments. For sampling, animals were euthanized by exsanguination following decapitation. All studies were reviewed and approved by the Institutional Animal Care and Use Committee (IACUC) of Takeda Pharmaceutical Company Limited, accredited by AAALAC (Association for Assessment and Accreditation of Laboratory Animal Care International) and the ethical approval reference numbers are AU-00020666 and AU-00020789.

2.3 | GCS activity assay using RapidFire mass spectrometry

The assay was performed in 384-well V-base polypropylene plates (Greiner Bio-One) with a final reaction volume of 10 μl. The compounds were added to plates in 100 nL aliquots in DMSO using the Echo 555 acoustic dispenser (Labcyte Inc.). The compounds were tested in triplicate using a threefold, 8-point serial dilution. GCS activity was assayed (Lipsky & Pagano, 1985) with slight modifications. Initially, 5 μl of a substrate solution containing C8-Ceramide liposome (15.6 mol % C8-ceramide (Avanti Polar Lipids Inc.) and 84.6 mol % dioleoylphosphatidylcholine, DOPC (NOF Corporation), and UDP-glucose (Fujifilm Wako) in the assay buffer (20 mM Tris, pH 7.5, 1 mM DTT, 0.01% Tween 20 and 0.01% BSA) was added to plates. A volume of 5 μl of an enzyme solution (25 μg/ml) in assay buffer was added to initiate the reaction. All additions were performed using a Multidrop Combi (Thermo Fisher Scientific). The plate was kept at 20-25°C for 1 h. To stop the reaction, 60 μl of 1% HCOOH containing 250 nM C18-d35 ceramide (Matreya LLC) as the internal standard in 75% isopropanol. For RapidFire mass analyses, 5 μl of the enzyme reaction solution was aspirated from the quenched assay plates and loaded onto a C18 solid-phase extraction (SPE) cartridge (Agilent Technologies) with a 70:30 (v/v) methanol–water solution containing 5 mM ammonium formate and 0.2% HCOOH for 2000 ms. The analytes were then eluted into the mass spectrometer using a 95:5 (v/v) methanol–water solution containing 5 mM ammonium formate and 0.2% HCOOH for 5000 ms. C8-Glycosyl ceramide and C18-d35 ceramide were detected using MRM with Q1/Q3 transitions at m/z 588.5 to 246.5 and m/z 762.9 to 265.5, respectively on Sciex API4000 triple quadrupole mass spectrometer (Applied Biosystems) in the positive electrospray ionization mode.

2.4 | RapidFire mass spectrometry data processing

The extracted ion chromatograms for each transition were integrated and processed using the RapidFire Integrator software. The

data for each well were normalized by monitoring product conversion with (Product) / (Internal standard) ratio. The compound activities were determined by plotting the percent inhibition data through normalization from 0% (DMSO only) and 100% inhibition (no-enzyme control) and modeling a four-parameter logistic fit to obtain IC_{50} values. The initial rates of GCS activity were determined by incubating GCS with various concentrations of ceramide and UDP-Glucose in assay buffer at 20-25°C for 60 min. The reaction product was measured using the RapidFire mass assay. The initial rates were fitted to the Michaelis-Menten equation to estimate the Km values. All curve fitting was performed by GraphPad Prism 6.07 for Windows.

2.5 | Equations

Steady-state kinetic data were fit globally to the following equations:

Noncompetitive inhibition

$$Y = Vmax * [S] / Km (1 + [I] / Ki) + [S](1 + [I] / alpha * Ki)$$

Uncompetitive inhibition

$$Y = Vmax * [S] / Km + [S](1 + [I] / alphaKi)$$

2.6 | Affinity selection mass spectrometry (AS-MS)

Various concentrations of T-036, venglustat, and eliglustat were incubated with 10 μg/ml microsomal protein-expressing GCS in 50 μl of assay buffer with 20 mM Tris–HCl (pH7.5), 1 mM DTT, and 0.01% Tween20 for 60 min at 20-25°C with 200 μM UDP-glucose or 70 μM C8-ceramide or neither. The reaction was terminated by a 96-well ultrafiltration membrane (MSHVN45, Millipore Corp) packed with Sephadex G50-Fine to separate the bound and free compounds. Next, 30 μl of the eluent was mixed with 100 μl of 70% acetonitrile to denature the enzyme–compound complexes. Free compounds were quantified using a LC/MS system (Agilent 6495 LC/MS/MS System) equipped with an electron spray ionization interface. Specific binding was calculated by subtracting the counts measured in the absence of GCS from those in the presence of GCS. T-036, venglustat, and eliglustat were separated on a reverse-phase column (Unison UK-C18, 3 μm, 30 × 2.0 mm; Imtakt) using a linear gradient at a flow rate of 0.7 ml/min. The mobile phase consisted of solvent A, 10 mM ammonium formate containing 0.2% formic acid, and solvent B, acetonitrile containing 0.2% formic acid. According to the gradient protocol, the gradient solution was 5% solvent B at 0 min, 95% solvent B at 0.1 to 0.5 min, and isocratic elution with 95% solvent B was continued for 1.9 min. Finally, the column was washed with 5% solvent B in solvent A for 0.5 min. The mass transitions (Q1/Q3) used for T-036, venglustat, and eliglustat was 461.15/363.1, 390.17/220, and 405.28/84.1, respectively.

2.7 | Preparation of T-036

T-036 was synthesized at Neuroscience Drug Discovery Unit in Takeda Pharmaceutical Company Limited. For in vivo experiment, T-036 was reconstituted with a 0.5% (w/v) methylcellulose solution (Fujifilm Wako) and was used at the indicated doses. The drug was administered to mice at 10 ml/kg body weight.

2.8 | Time course PD/PK study

Eighty 9-week-old male C57BL/6J mice were divided into 16 groups (5 mice per group), and vehicle or T-036 was treated for each time point (0.5, 1, 2, 4, 8, 16, 24, and 48 h). After the drug administration, the mice were killed to collect their cerebral cortex and plasma. The samples were frozen and stored at −80°C until analysis.

2.9 | Dose-dependent study

Thirty-five 7-week-old male C57BL/6J mice were divided into 7 groups (5 mice per group), and vehicle or T-036 at 1 to 300 mg/kg was administered. The mice were killed 6 h after the administration to collect their cerebral cortex and plasma. The samples were frozen and stored at −80°C until analysis.

2.10 | Evaluation of GlcCer and GlcSph in the GD mouse model

In the single administration, 18 15-week-old male Gba D409V KI mice were divided into 3 groups (6 mice per group), and vehicle or T-036 at 10 or 30 mg/kg was administered. The mice were sacrificed 6 h after the administration to collect their cerebral cortex and plasma. In the repetitive administration, 15 20-week-old male Gba D409V KI mice were divided into 3 groups (5 mice per group), and vehicle or the drug at 10 or 30 mg/kg was orally administered once daily for 2 months. The mice were killed at 2 h after the last administration to collect their cerebral cortex and plasma. The samples were frozen and stored at −80°C until analysis.

2.11 | Measurement of T-036, GlcCer, and GlcSph concentrations in plasma and cerebral cortex

GlcCer and GlcSph were quantified according to Boutin and Hamler et al (Boutin et al., 2016; Hamler et al., 2017) with modifications. The cerebral cortex was homogenized immediately after collection in 4 volumes of MeOH on ice. The concentrations of T-036, glucosylceramide, and GlcSph in the supernatant of plasma and the homogenate of the cerebral cortex were quantitated by spectral analysis under the multiple reaction monitoring modes

with an API-4000 or API-5000 triple-quadrupole mass spectrometer (AB Sciex) interfaced with the Prominence UFLC system (Shimadzu).

2.12 | Determination of unbound fractions in brain and plasma in mice

An equilibrium dialysis method was used to estimate unbound fraction of test compound in the plasma and brain of mice (Sato et al., 2020). In brief, the test compound was spiked at 1 μM into the plasma, the 20% (w/v) brain homogenate, or 100 mM sodium phosphate buffer. The spiked samples were then transferred into an equilibrium dialysis apparatus at 37°C for 16–20 h. The concentration of unbound test compound in the plasma, the brain homogenate, or the buffer obtained from the apparatus was determined by LC-MS/MS. The unbound fraction in the brain ($f_{u,brain}$) was calculated using the following equation:

$$f_{u,brain} = \frac{1}{D \times \left(\frac{1}{f_{u,brain}'} - 1\right) + 1}$$

where D and $f_{u,brain}'$ represent the dilution factor of brain homogenate and unbound fraction determined in the 20% (w/v) brain homogenate, respectively.

2.13 | Quantification and statistical analysis

Statistical analysis was performed using EXSUS (CAC EXICARE Corporation). In the dose–response studies, Bartlett's test was performed to assess the homogeneity of variances, followed by two-tailed Williams' test (for parametric data: $p > 0.05$ by Bartlett's test) or two-tailed Shirley-Williams test (for nonparametric data: $p < 0.05$ by Bartlett's test) for comparing dose-dependent effects of multiple doses of the test compounds with the control group. Differences yielding p values <0.05 were considered significant. In our studies, no sample size calculation was performed, however, 5 or 6 animals per group were used because this number was considered appropriate to evaluate significant difference between the control and the drug treatments based on the previous reports (Cabrera-Salazar et al., 2012; Marshall et al., 2019).

2.14 | Study design

This nonclinical exploratory study was not preregistered, no exclusion criteria were pre-determined, no animals were excluded, and no outliers were identified / excluded. No randomization was performed to allocate subjects: For example, in the case of Figure 5, the mice were unintentionally numbered, and then assigned in order into three groups (i.e. ABCABCABC…). No blinding was performed in the study.

3 | RESULTS

3.1 | T-036 is a novel, potent GCS inhibitor with unique characteristics

Our study focused on discovering a new class of GCS inhibitors. We developed an enzymatic assay to measure the GlcCer formation activity of GCS. We screened a series of novel synthetic compounds and identified T-036, a potent inhibitor with an IC_{50} value of 31 nM (Figure 1 and Table S2). T-036 had a novel chemical structure distinct from substrate mimetic inhibitors that harbor an aliphatic amine moiety.

We characterize T-036 by examining its binding to GCS in the presence of GCS substrates using AS-MS and GCS enzymatic reaction. The binding of T-036 to GCS was detected through AS-MS in the presence or absence of UDP-glucose (Figure 2a). We then performed a steady-state kinetic competition experiment by measuring GCS activity in the presence of T-036 and various UDP-glucose concentrations; then, we globally fitted the data to a noncompetitive inhibition model (Figure 2b). The Lineweaver-Burk plots of T-036 displayed a characteristic pattern of intersecting lines (Figure 2c). These data indicate that T-036 inhibits GCS via noncompetitive binding against UDP-glucose.

Next, we characterized other GCS inhibitors, venglustat and eliglustat, for comparison. Miglustat was not subjected to the AS-MS and steady-state kinetic competition experiment as its enzymatic inhibition was not as potent as the others (Table S2). The results showed their binding to be different from that of T-036. The binding of venglustat and eliglustat to GCS was not detected in the absence of UDP-glucose; they bind GCS in the presence of UDP-glucose (Figure 2d and g). A steady-state kinetic GCS competition experiment was conducted, and the data globally fitted to an uncompetitive inhibition model (Figure 2e and h). The Lineweaver-Burk plots of venglustat and eliglustat displayed lines characteristic of uncompetitive inhibition (Figure 2f and I). These data indicated that the inhibition of GCS by venglustat and eliglustat was uncompetitive against UDP-glucose. Kinetic parameters in the steady-state competition assay are summarized in Table 1. Vmax, Km, and Ki were 39.86 ± 0.31 μmol/min, 3.02 ± 0.31 μM, and 16.44 ± 1.70 μM, respectively.

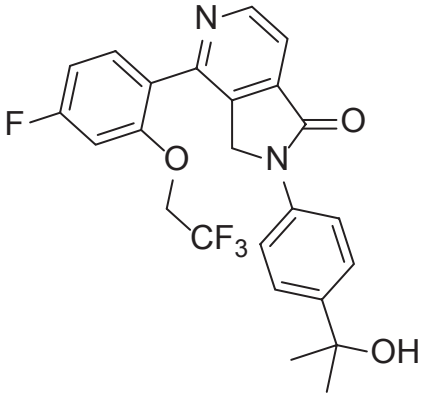

T-036

FIGURE 1 Chemical structure of T-036

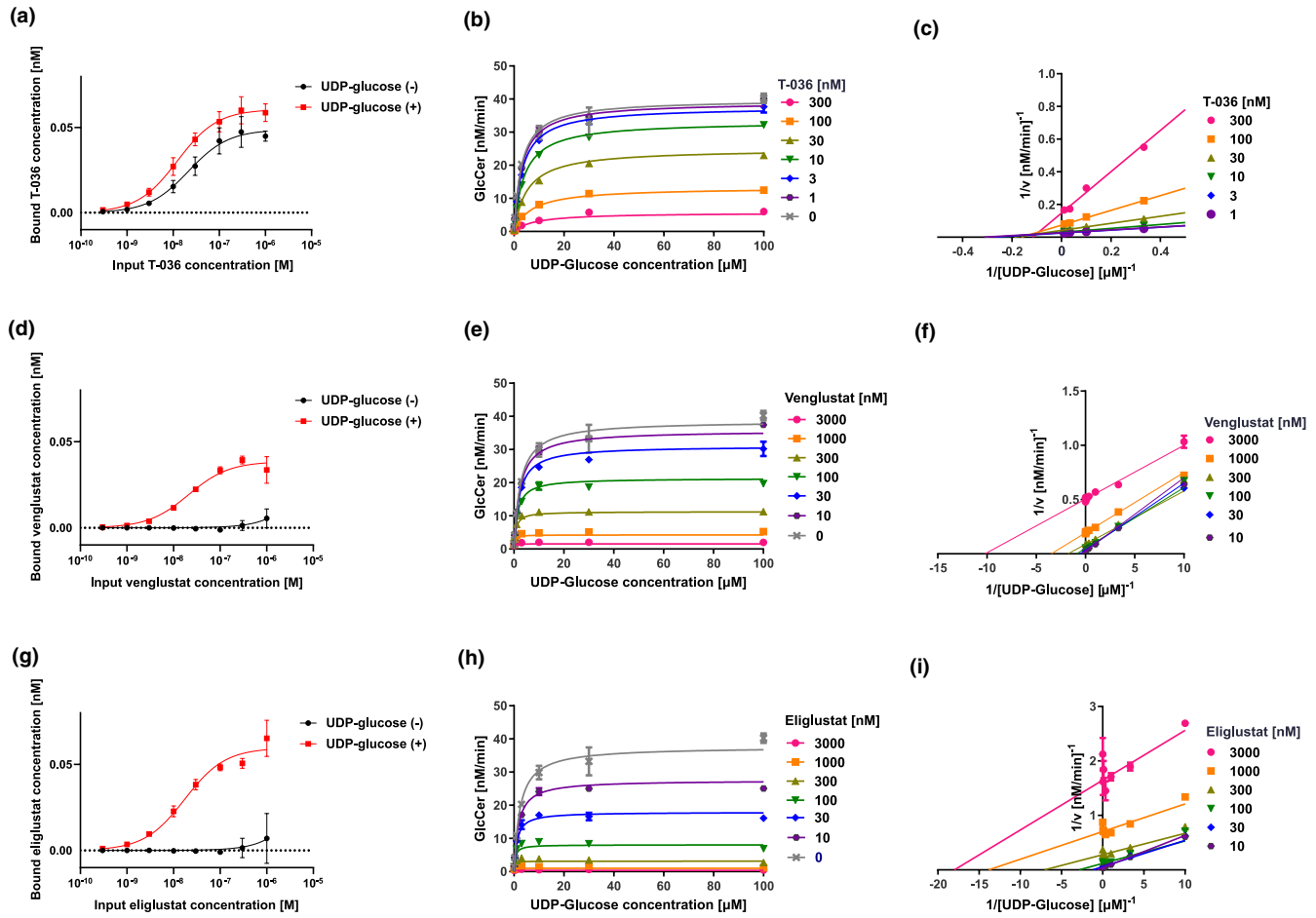

FIGURE 2 Affinity of T-036, venglustat, and eliglustat to GCS with or without UDP-glucose assessed by AS-MS and Steady-State Kinetic Analysis. (a) Binding assay of T-036 to GCS with or without UDP-glucose using affinity-selection mass spectrometry. (b) Steady-state kinetic analysis of T-036 inhibition of GCS activity using glucosylceramide synthase assay at various UDP-glucose concentrations. Curves are globally fit to a noncompetitive inhibition model. $R^2 = 0.9932$. (c) Plot of 1/v vs 1/[UDP-glucose] at a fixed ceramide concentration (7.4 μM) and various concentrations of T-036 shows noncompetitive inhibition. (d) Binding assay of venglustat to GCS with or without UDP-glucose using affinity-selection mass spectrometry. (e) Steady-state kinetic analysis of venglustat inhibition of GCS activity using glucosylceramide synthase assay at various UDP-glucose concentrations. Curves are globally fit to an uncompetitive inhibition model. $R^2 = 0.9893$. (f) Plot of 1/v vs 1/[UDP-glucose] at a fixed ceramide concentration (7.4 μM) and various concentrations of venglustat shows uncompetitive inhibition. (g) Binding assay of eliglustat to GCS with or without UDP-glucose using affinity-selection mass spectrometry. (h) Steady-state kinetic analysis of eliglustat inhibition of GCS activity using glucosylceramide synthase assay at various UDP-glucose concentrations. Curves are globally fit to an uncompetitive inhibition model. $R^2 = 0.9869$. (i) Plot of 1/v vs 1/[UDP-glucose] at a fixed ceramide concentration (7.4 μM) and various concentrations of eliglustat shows uncompetitive inhibition. Data are presented as the mean ± SD, $n = 3$ (n = number of reactions)

TABLE 1 Kinetic parameters of GCS inhibition of T-036, venglustat, and eliglustat for UDP-glucose

Compound	V_{max} (μmol min^{-1})	K_m (μM)	K_i (μM)
T–036	39.86 ± 0.31	3.02 ± 0.11	16.44 ± 1.70
Venglustat	38.58 ± 0.32	2.53 ± 0.09	–
Eliglustat	37.60 ± 0.45	2.37 ± 0.11	–

Data are presented as the mean ± *SD* ($n = 3$; n = number of reactions).

The inhibition of GCS by the three inhibitors in the presence of ceramide, the other substrate of GCS, was analyzed with a steady-state kinetic GCS competition experiment. Again, the data were globally fitted to a noncompetitive inhibition model (Figure S2b, e, and h; Table S3). The Lineweaver-Burk plots displayed a pattern of intersecting lines characteristic of a noncompetitive inhibition (Figure S2c, f, and i), indicating that the inhibition of GCS by T-036, venglustat, and eliglustat were also noncompetitive against ceramide.

3.2 | In vivo pharmacodynamics (PD) / pharmacokinetics (PK) study of T-036 in mice

For an in vivo evaluation of T-036, we first characterized its PK profile. After a single oral administration at 10 mg/kg to normal mice, the amount of T-036 in cerebral cortex and plasma reached a peak concentration (Cmax) of 1677 ng/g tissue and 3972 ng/ml at approximately 1.1 and 0.9 h, respectively (Table 2), suggesting that the compound has good bioavailability and brain penetration.

Then, PD effect of T-036 was evaluated by examining the time-course change of GlcCer. GlcCer concentrations in the cerebral cortex and plasma of normal mice were measured at 0.5, 1, 2, 4, 8, 16, 24, and 48 h after the single oral administration of T-036 at 10 mg/kg or vehicle (Figure 3). The reduction in GlcCer concentration in the cerebral cortex and plasma by T-036 showed similar time-course patterns; maximal effects in the cerebral cortex and plasma were observed at 16 and 8 h, respectively. In addition, T-036 decreased GlcCer concentration in a dose-dependent manner at 1, 3, 10, 30, 100, and 300 mg/kg at 6 h after administration, which was significant from 10 and 1 mg/kg in the cerebral cortex and plasma, respectively ($p < 0.0001$) (Figure 4). Although the dose-dependent exposure of T-036 was confirmed (Table S4), the reduction in GlcCer concentration reached a plateau at 300 mg/kg or a lower dose. Relative amounts at 300 mg/kg were 40 ± 3% and 50 ± 4% compared with the vehicle treatment in the cerebral cortex and plasma, respectively.

TABLE 2 The pharmacokinetic parameters of T-036 in cerebral cortex and plasma of normal mice after a single oral administration T-036 at 10 mg/kg

Parameters	Cerebral cortex	Plasma
MRT (h)	7.3	8.1
T_{max} (h)	1	1
C_{max} (ng/g or ng/ml)	1605	3845
AUC (ng·h/g or ng·h/ml)	13 197	37 950

Data are presented as the mean ($n = 5$; n = number of animals).

3.3 | GlcCer and GlcSph reduction by T-036 in GD mouse model

As the GlcSph level is considered a key surrogate marker for GD progression, the effect of T-036 on the GlcSph level was examined in the GD model Gba D409V KI mice. GlcSph elevation in the cerebral cortex of Gba D409V KI mice compared with WT was observed (Figure S3) and is consistent with the previous report (Ikuno et al., 2019). The doses of 10 and 30 mg/kg were selected because of their significant PD effects in the cerebral cortex observed in the dose-dependent study (Figure 4). The single administration of T-036 at 10 or 30 mg/kg to Gba D409 KI mice significantly reduced GlcCer, but not GlcSph, in the cerebral cortex and plasma (Figure 5b–e). Relative levels of brain GlcCer to the vehicle treatment were 55 ± 2% (mean ± SEM, $p < 0.0001$) and 41 ± 2% (mean ± SEM, $p < 0.0001$) at 10 and 30 mg/kg, respectively (Figure 5d), and relative levels of plasma GlcCer were 85 ± 1% (mean ± SEM, $p = 0.0007$) and 79 ± 3% (mean ± SEM, $p < 0.0001$) at 10 and 30 mg/kg, respectively (Figure 5e). By contrast, relative levels of brain GlcSph were 89 ± 7% (mean ± SEM, $p = 0.2348$) and 80 ± 2% (mean ± SEM, $p = 0.0310$) at 10 and 30 mg/kg, respectively (Figure 5b), and levels of plasma GlcSph were 99 ± 6% (mean ± SEM, $p = 0.4718$) and 88 ± 4% (mean ± SEM, $p = 0.2011$) at 10 and 30 mg/kg, respectively (Figure 5c). Then, we tested T-036 in a 2-month treatment study. No obvious adverse events were observed throughout the treatment, suggesting that T-036 was well-tolerated at 10 and 30 mg/kg. T-036, at 10 and 30 mg/kg, reduced GlcSph in the cerebral cortex and plasma in a dose-dependent manner. Significance was detected at 30 and 10 mg/kg or higher in the cerebral cortex and

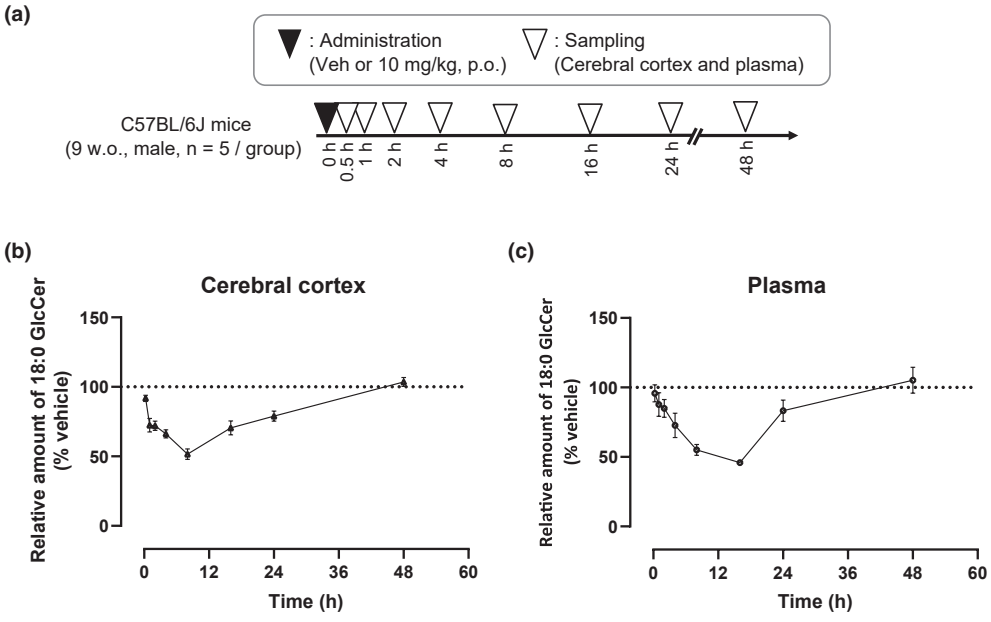

FIGURE 3 Time course study of GlcCer reduction by T-036 in normal mice. The graphical experimental scheme of the study is shown (a). C57BL/6J mice were orally administrated with vehicle or T-036 (10 mg/kg). Cerebral cortex and plasma from the mice were collected at 0.5, 1, 2, 4, 8, 16, 24, and 48 h after the administration. Relative amount of glucosylceramide (GlcCer) comparing to vehicle at each time point in cerebral cortex (b) and plasma (c) was measured. Data are presented as the mean ± SEM ($n = 5$; n = number of animals)

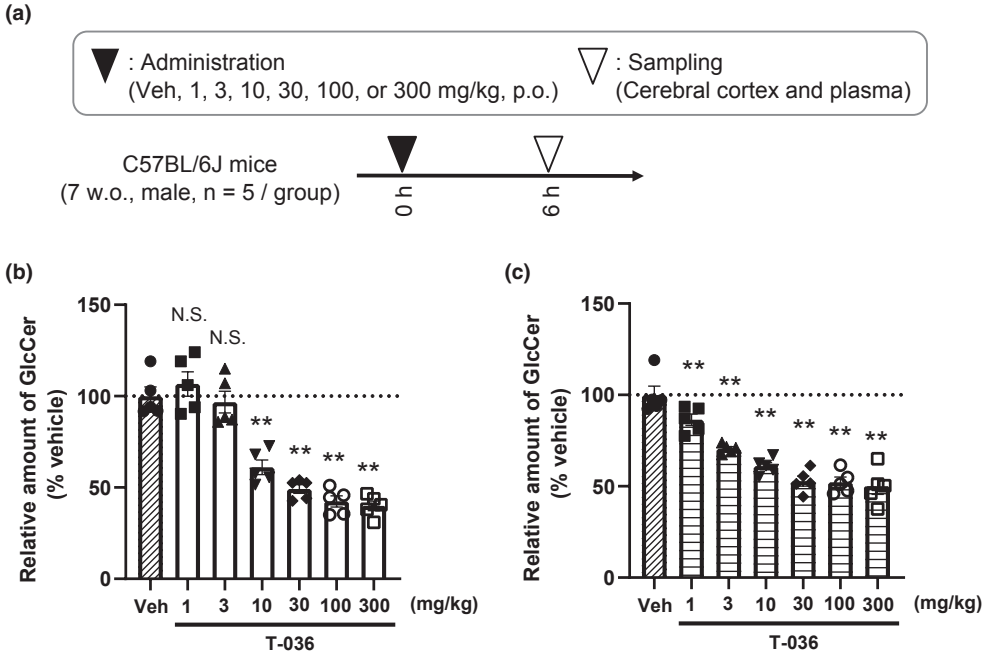

FIGURE 4 Dose dependency of GlcCer reduction by T-036 in normal mice. The graphical experimental scheme of the study is shown (a). C57BL/6J mice were orally administrated with vehicle (veh) or T-036 (1, 3, 10, 30, 100, and 300 mg/kg). Plasma and cerebral cortex from the mice were collected at 6 h after administration. Relative amount of glucosylceramide (GlcCer) comparing to vehicle in cerebral cortex (b) and plasma (c). Data are presented as the scatter plots and the mean ± SEM ($n = 5$; n = number of animals). $^{**}p < 0.01$ in two-tailed Williams' test, N.S., not significant

plasma, respectively (Figure 5f and g). Relative levels of brain GlcSph were 73 ± 6% (mean ± SEM, $p = 0.0283$) and 61 ± 1% (mean ± SEM, $p = 0.0053$) at 10 and 30 mg/kg, respectively (Figure 5f), and levels of plasma GlcSph were 58 ± 6% (mean ± SEM, $p = 0.0001$) and 36 ± 3% (mean ± SEM, $p < 0.0001$) at 10 and 30 mg/kg, respectively (Figure 5g). Reductions in GlcCer were also confirmed and reduction in plasm more robust than that in single-dose treatment (Figure 5e and i). Relative levels of brain GlcCer were 58 ± 2% (mean ± SEM, $p < 0.0001$) and 40 ± 3% (mean ± SEM, $p < 0.0001$) at 10 and 30 m g/kg, respectively (Figure 5h), and relative levels of plasma GlcCer were 40 ± 4% (mean ± SEM, $p < 0.0001$) and 21 ± 2% (mean ± SEM, $p < 0.0001$) at 10 and 30 mg/kg, respectively (Figure 5i).

4 | DISCUSSION

Here, we have discovered and evaluated T-036, a novel CNS-penetrant GCS inhibitor that does not harbor an aliphatic amine moiety, unlike the existing GCS inhibitors.

We clarified that T-036 binds to GCS independently of the concentration of GCS substrates, i.e., UDP-glucose and ceramide, and inhibits GCS in a noncompetitive mode against the substrates (Figure 2 and Figure S2). Since noncompetitive inhibition is relevant to bind a molecule to an allosteric site of an enzyme (Delaune & Alsayouri, 2020), T-036 may bind to the allosteric site of GCS, which is distinct from substrate binding sites of GCS.

By contrast, the existing GCS inhibitors, such as venglustat and eliglustat, do not bind to GCS without UDP-glucose and inhibit GCS in an uncompetitive mode against UDP-glucose. Also, they show a noncompetitive inhibition mode against ceramide. Therefore, T-036 has a unique chemical structure and binding property to GCS distinct from those of the existing GCS inhibitors. Moreover, the noncompetitive inhibition mode of T-036 against UDP-glucose may result in a significant advantage over the uncompetitive inhibition mode of other inhibitors because it enables T-036 to bind and inhibit GCS regardless of the concentration of UDP-glucose, an activated form of glucose, whose cerebral metabolic rates could be perturbed in Gaucher disease (Kono et al., 2010).

In in vivo pharmacological evaluation, single oral dosing of T-036 showed a reduction of GlcCer level in the cerebral cortex and plasma. GlcCer is directly synthesized from ceramide and UDP-glucose by GCS; therefore, the GlcCer level could be a PD marker of the GCS inhibitor. Membrane permeability of T-036 was confirmed by PAMPA: 313 and 247 nm/s in pH5.0 and 7.4, respectively, which are expected to penetrate plasma membrane and suppress intracellular GlcCer synthesis in the neurons and/or glial cells. Our time-course studies of PK and PD indicate hysteresis in the PK/PD relationship. Namely, the maximal PD change was observed followed by the T_{max} of the compound concentration (Table 2 and Figure 3); this might be due to the turnover rate of GlcCer. In fact, the half-life of GlcCer in vivo was reported to be 6 h (Skotland et al., 2016).

Also, the PK data of T-036 clearly shows brain penetration and the brain:plasma ratio of the compound is calculated as 0.35. Therefore, the brain penetration of T-036 should contribute to the reduction of GlcCer in the brain as eliglustat, which does not

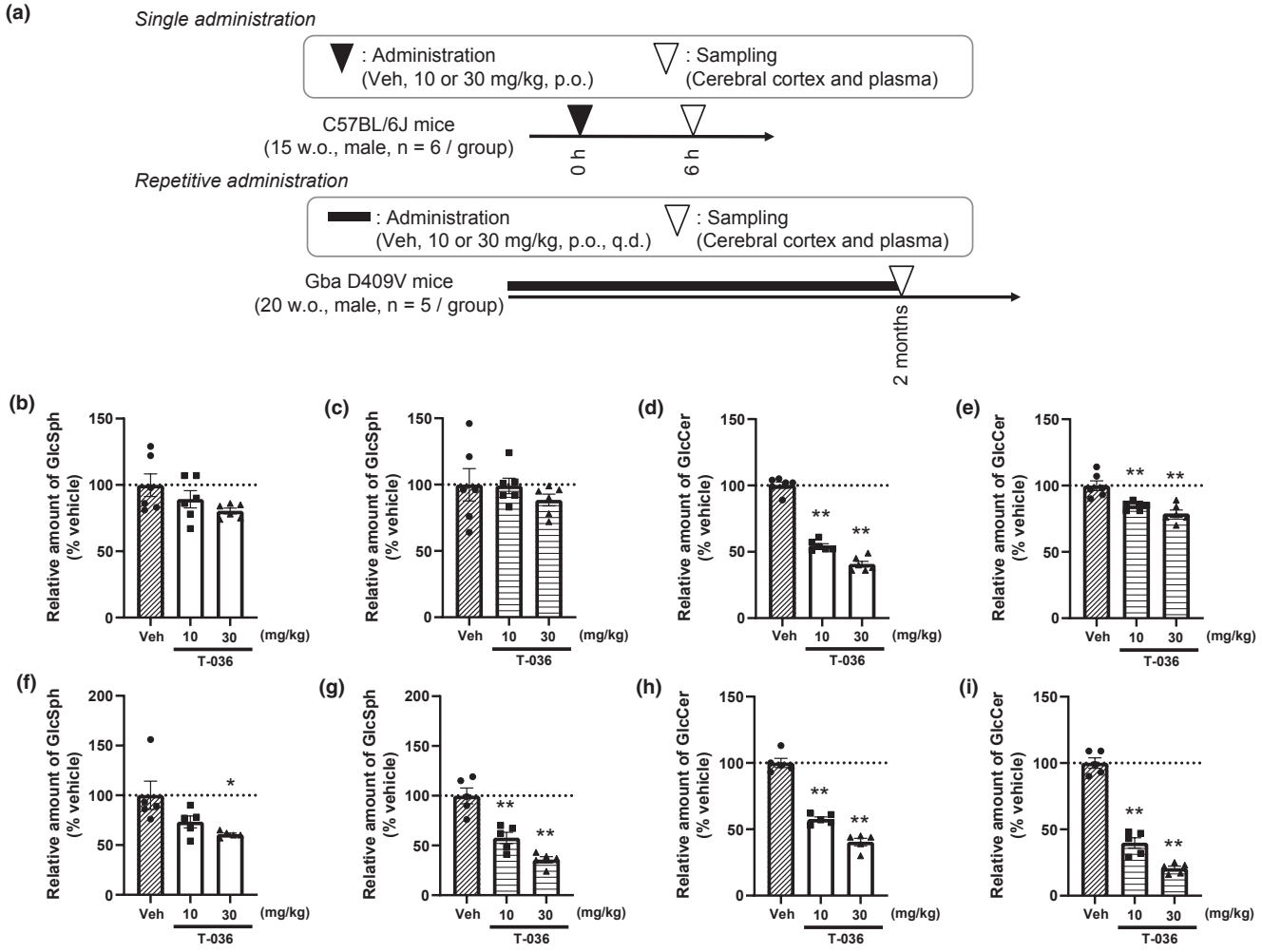

FIGURE 5 GlcCer and GlcSph reduction by T-036 in GD mouse model. The graphical experimental scheme of the study is shown (a). (b–e) Gba D409V KI mice were orally administrated with vehicle (veh) or T-036 (10, 30 mg/kg) for 1 day. The concentrations of glycosphingolipids were measured in cerebral cortex (b and d) and plasma (c and e). Data shows the relative amount of GlcSph (b and c) and GlcCer (d and e) comparing to vehicle. Data are presented as the scatter plots and the mean ± SEM ($n = 6$; n = number of animals). $^{*}p < 0.05$, $^{**}p < 0.01$ in two-tailed Williams' test. (f–i) Gba D409V KI mice were orally administrated with vehicle or T-036 (10, 30 mg/kg) for 2 months. The concentrations of glycosphingolipids were measured in cerebral cortex (f, h) and plasma (g, i). Data shows the relative amount of GlcSph (f, g) and GlcCer (h, i) comparing to vehicle. Data are presented as scatter plots and the mean ± SEM ($n = 5$; n = number of animals). $^{*}p < 0.05$, $^{**}p < 0.01$ in two-tailed Williams' test

penetrate CNS, has no significant effect on the GlcCer level in the brain (Larsen et al., 2012). In addition to PK, unbound fraction of the compound in brain homogenate (Fu,b) and plasma (Fu,p) were determined: Fu,b and Fu,p are 0.027 and 0.18, respectively. Therefore, active exposure concentration in the brain at 10 mg/kg and in the plasma at 1 mg/kg is calculated to be about 45 nM and 167 nM, respectively, exceeding the IC_{50} value and accounting for a significant effect on the level of GlcCer.

Next, effect of T-036 on GlcSph, which plays a role in GD progression and is elevated in the GD model, was tested in Gba D409V KI mice. GlcCer in the cerebral cortex and plasma was significantly reduced by the single dosing of T-036. However, effect of T-036 on the plasma GlcCer was smaller than that in the cerebral cortex and less than that in normal mice. As GlcCer is metabolized to ceramide and glucose by glucocerebrosidase, its activity is considered the rate-limiting step in GlcCer reduction by GCS inhibition. Impaired glucocerebrosidase activity by mutant Gba KI may weaken efficacy in the plasma of D409V KI mice. The study that reports that glucocerebrosidase activity is relatively spared in the brain compared with that in the peripheral tissues in the KI mice (Xu et al., 2003) is consistent with our observation. In the chronic dosing, the reduction in GlcCer was more robust than that by the single administration especially in plasma. GlcCer was reduced by 60% and 79% in the brain and plasma, respectively, suggesting that GlcCer production is mainly contributed to by GCS. Similar result by using a different GCS inhibitor is reported (Richards et al., 2012).

Unlike GlcCer, GlcSph was not significantly affected by the acute administration of T-036 in either the cerebral cortex or plasma. On the other hand, multiple administrations of T-036 for 2 months significantly reduced GlcSph. GlcSph is generated from GlcCer by

N-acylsphingosineamidohydrolase 1 and degraded by glucocerebrosidase (Lin et al., 2019); therefore, the effect of GCS inhibition on GlcSph level is indirect, and the suppression of GlcSph level by GCS inhibitor could be slower than that of GlcCer. As there has been no approved medication for neurological symptoms of GD, it is unknown how much reduction of GlcSph is required to achieve therapeutic benefit. However, the approved GCS inhibitor eliglustat has shown a therapeutic effect in peripheral pathologies such as splenomegaly in the clinical trial and reduces GlcSph concentration in the plasma by 40% at that dose (Mistry et al., 2017). Therefore, it can be assumed that a 40% reduction of the GlcSph level in the brain improves central nervous system symptoms of GD. In our study, T-036 could achieve a similar extent of reduction in the brain at 30 mg/kg, indicating that T-036 may be effective in treating neuropathic GD. Because GBA activating compounds have been reported to reduce GSLs (Burbulla et al., 2019), we tested whether T-036 affect GBA activity. T-036 does not either activate or inhibit GBA in our cell-free assay (Table S2). Therefore, reduction of GlcCer by T-036 can be accounted for by GCS inhibition mainly.

Recently some GCS inhibitors with brain penetration have been reported. They significantly reduced brain GlcSph in GD models at a level similar to T-036. Moreover, they affect downstream pathway, such as neuroinflammation and the accumulation of α-synuclein (Cabrera-Salazar et al., 2012; Marshall et al., 2016; Sardi et al., 2017). These observations support the idea that GlcSph reduction by T-036 could provide therapeutic benefits to neuropathic GD. While the reported molecules venglustat and GZ667161 are thought to belong to the same chemical series and harbor an aliphatic amine moiety, T-036 has a completely new chemical structure. Additionally, the accumulation of other GSLs such as GM2 and GM1 is known to cause various LSDs (Polo et al., 2017). GM2 accumulation results in Tay-Sachs disease or Sandhoff disease, and GM1 is associated with GM1 gangliosidosis. T-036 significantly reduced these downstream GSLs. Therefore, T-036 is also expected to have therapeutic potential for other diseases. On the other hand, decrease in GSLs by GCS could lead to various biological effects besides therapeutic effects. For example, it is reported that depletion of GM1 by GCS inhibitor $_{D}$-PDMP negatively regulates NGF-induced TrK signaling in the cellular study (Mutoh et al., 1998). In addition, our lipidomics profiling indicates that increase in ceramide and sphingomyelin as well as alteration in diacylglycerol and triacylglycerol by the chronic treatment of T-036 in the Gba D409V KI mice (Table S5 and Figure S5). Hence, it may be required to carefully assess risk and benefit of GCS inhibitor in the future clinical examination.

In summary, T-036 is the novel GCS inhibitor with chemical features distinct from the reported compounds. T-036 is orally available and brain-penetrant; it is expected to be effective on neuropathic GD, which cannot be treated by currently available medications. The in vitro and in vivo data in this study indicate that T-036 is a promising lead compound for the treatment of GD.

ACKNOWLEDGMENTS

We thank M. Inazuka and H. Matsui for their valuable discussion. We thank that M. Miyabayashi and K. Ogawa for help with the in vivo study. Y. Zama for preparation of microsomal protein. Without their contribution, this study would not have been possible. We thank all members of this project team at Takeda for their contribution. The animals were supplied by Axcelead Drug Discovery Partners, Inc. and HAMRI CO., LTD. The lipid measurement (GM3, GM2, GM1, GD3, and GD1) was conducted by Axcelead Drug Discovery Partners, Inc.

Funding information: This work was supported by Takeda Pharmaceutical Company Limited.

All experiments were conducted in compliance with the ARRIVE guidelines.

CONFLICT OF INTEREST

T.F., Y.T., S.S., Y.T., T.M, and T.O. are employed by Takeda Pharmaceutical Company Limited. H.O., S.S., and T.M are employed by Axcelead Drug Discovery Partners. T-036, which was used in this study, is a discovered tool molecule and is not commercially available from either companies. Synthesis method is available from WO2021020363.

AUTHORS CONTRIBUTIONS

T.F. and T.O. wrote the main manuscript text, performed the statistical analysis, and prepared figures. T.F. performed in vivo study. Y.T. and Y.T. synthesized T-036. H.O. supervised the GCS activity assay and Affinity Selection Mass Spectrometry. S.S. Performed the GCS activity assay. T.M. performed Affinity Selection Mass Spectrometry. S.S. performed Lipid analysis. Y.T. and T.F. organized this project. M.T. and T.O. were responsible for the overall the project.

Open Research

DATA AVAILABILITY STATEMENT

All raw data are available from the corresponding author upon request.

ORCID

Yuta Tanaka https://orcid.org/0000-0002-6110-7990
Tomohiro Onishi https://orcid.org/0000-0003-0633-9323

REFERENCES

Abe, A., Radin, N. S., Shayman, J. A., Wotring, L. L., Zipkin, R. E., Sivakumar, R., Ruggieri, J. M., Carson, K. G., & Ganem, B. (1995). Structural and stereochemical studies of potent inhibitors of glucosylceramide synthase and tumor cell growth. *Journal of Lipid Research*, 36, 611–621. https://doi.org/10.1016/S0022-2275(20)39895-3.

Alaei, M. R., Tabrizi, A., Jafari, N., & Mozafari, H. (2019). Gaucher disease: New expanded classification emphasizing neurological features. *Iranian Journal of Child Neurology*, 13, 7–24.

Ashe, K. M., Budman, E., Bangari, D. S., Siegel, C. S., Nietupski, J. B., Wang, B., Desnick, R. J., Scheule, R. K., Leonard, J. P., Cheng, S. H., & Marshall, J. (2015). Efficacy of enzyme and substrate reduction therapy with a novel antagonist of glucosylceramide synthase for Fabry disease. *Molecular Medicine*, 21, 389–399.

Boutin, M., Sun, Y., Shacka, J. J., & Auray-Blais, C. (2016). Tandem mass spectrometry multiplex analysis of glucosylceramide and Galactosylceramide isoforms in brain tissues at different stages of Parkinson disease. *Analytical Chemistry*, 88, 1856–1863.

Burbulla, L. F., Jeon, S., Zheng, J., Song, P., Silverman, R. B., & Krainc, D. (2019). A modulator of wild-type glucocerebrosidase improves

pathogenic phenotypes in dopaminergic neuronal models of Parkinson's disease. *Science Translational Medicine*, 11, eaau6870. https://doi.org/10.1126/scitranslmed.aau6870.

Cabrera-Salazar, M. A., Deriso, M., Bercury, S. D., Li, L., Lydon, J. T., Weber, W., Pande, N., Cromwell, M. A., Copeland, D., Leonard, J., Cheng, S. H., & Scheule, R. K. (2012). Systemic delivery of a glucosylceramide synthase inhibitor reduces CNS substrates and increases lifespan in a mouse model of type 2 Gaucher disease. *PLoS One*, 7, e43310. https://doi.org/10.1371/journal.pone.0043310.

Cox, T. M., Aerts, J. M., Andria, G., Beck, M., Belmatoug, N., Bembi, B., Chertkoff, R., Vom Dahl, S., Elstein, D., Erikson, A., Giralt, M., Heitner, R., Hollak, C., Hrebicek, M., Lewis, S., Mehta, A., Pastores, G. M., Rolfs, A., Sa Miranda, M. C., & Zimran, A. (2003). The role of the iminosugar N-butyldeoxynojirimycin (miglustat) in the management of type I (non-neuronopathic) Gaucher disease: a position statement. *Journal of Inherited Metabolic Disease*, 26, 513–526.

Dekker, N., van Dussen, L., Hollak, C. E., Overkleeft, H., Scheij, S., Ghauharali, K., van Breemen, M. J., Ferraz, M. J., Groener, J. E., Maas, M., Wijburg, F. A., Speijer, D., Tylki-Szymanska, A., Mistry, P. K., Boot, R. G., & Aerts, J. M. (2011). Elevated plasma glucosylsphingosine in Gaucher disease: relation to phenotype, storage cell markers, and therapeutic response. *Blood*, 118, e118–127. https://doi.org/10.1182/blood-2011-05-352971.

Delaune, K. P., & Alsayouri, K. (2020). Physiology, Noncompetitive Inhibitor. In StatPearls (Treasure Island (FL)).

Gu, X., Gupta, V., Yang, Y., Zhu, J. Y., Carlson, E. J., Kingsley, C., Tash, J. S., Schonbrunn, E., Hawkinson, J., & Georg, G. I. (2017). Structure-activity studies of N-Butyl-1-deoxynojirimycin (NB-DNJ) analogues: Discovery of potent and selective aminocyclopentitol inhibitors of GBA1 and GBA2. *Medicinal Chemistry*, 12, 1977–1984.

Hamler, R., Brignol, N., Clark, S. W., Morrison, S., Dungan, L. B., Chang, H. H., Khanna, R., Frascella, M., Valenzano, K. J., Benjamin, E. R., & Boyd, R. E. (2017). Glucosylceramide and glucosylsphingosine quantitation by liquid chromatography-tandem mass spectrometry to enable in vivo preclinical studies of neuronopathic gaucher disease. *Analytical Chemistry*, 89, 8288–8295.

Ikuno, M., Yamakado, H., Akiyama, H., Parajuli, L. K., Taguchi, K., Hara, J., Uemura, N., Hatanaka, Y., Higaki, K., Ohno, K., Tanaka, M., Koike, M., Hirabayashi, Y., & Takahashi, R. (2019). GBA haploinsufficiency accelerates alpha-synuclein pathology with altered lipid metabolism in a prodromal model of Parkinson's disease. *Human Molecular Genetics*, 28, 1894–1904.

Kono, S., Ouchi, Y., Terada, T., Ida, H., Suzuki, M., & Miyajima, H. (2010). Functional brain imaging in glucocerebrosidase mutation carriers with and without parkinsonism. *Movement Disorders*, 25, 1823–1829. https://doi.org/10.1002/mds.23213.

Larsen, S. D., Wilson, M. W., Abe, A., Shu, L., George, C. H., Kirchhoff, P., Showalter, H. D., Xiang, J., Keep, R. F., & Shayman, J. A. (2012). Property-based design of a glucosylceramide synthase inhibitor that reduces glucosylceramide in the brain. *Journal of Lipid Research*, 53, 282–291. https://doi.org/10.1194/jlr.M021261.

Lin, G., Wang, L., Marcogliese, P. C., & Bellen, H. J. (2019). Sphingolipids in the pathogenesis of Parkinson's disease and parkinsonism. *Trends in Endocrinology and Metabolism*, 30, 106–117.

Lipsky, N. G., & Pagano, R. E. (1985). Intracellular translocation of fluorescent sphingolipids in cultured fibroblasts: endogenously synthesized sphingomyelin and glucocerebroside analogues pass through the Golgi apparatus en route to the plasma membrane. *Journal of Cell Biology*, 100, 27–34. https://doi.org/10.1083/jcb.100.1.27.

Marshall, J., Nietupski, J. B., Park, H., Cao, J., Bangari, D. S., Silvescu, C., Wilper, T., Randall, K., Tietz, D., Wang, B., Ying, X., Leonard, J. P., & Cheng, S. H. (2019). Substrate reduction therapy for sandhoff disease through inhibition of glucosylceramide synthase activity. *Molecular Therapy*, 27, 1495–1506.

Marshall, J., Sun, Y., Bangari, D. S., Budman, E., Park, H., Nietupski, J. B., Allaire, A., Cromwell, M. A., Wang, B., Grabowski, G. A., Leonard, J. P., & Cheng, S. H. (2016). CNS-accessible inhibitor of glucosylceramide synthase for substrate reduction therapy of neuronopathic gaucher disease. *Molecular Therapy*, 24, 1019–1029.

McEachern, K. A., Fung, J., Komarnitsky, S., Siegel, C. S., Chuang, W. L., Hutto, E., Shayman, J. A., Grabowski, G. A., Aerts, J. M., Cheng, S. H., Copeland, D. P., & Marshall, J. (2007). A specific and potent inhibitor of glucosylceramide synthase for substrate inhibition therapy of Gaucher disease. *Molecular Genetics and Metabolism*, 91, 259–267.

Mistry, P. K., Lukina, E., Ben, T. H., Shankar, S. P., Baris, H., Ghosn, M., Mehta, A., Packman, S., Pastores, G., Petakov, M., Assouline, S., Balwani, M., Danda, S., Hadjiev, E., Ortega, A., Gaemers, S. J. M., Tayag, R., & Peterschmitt, M. J. (2017). Outcomes after 18 months of eliglustat therapy in treatment-naive adults with Gaucher disease type 1: The phase 3 ENGAGE trial. *American Journal of Hematology*, 92, 1170–1176.

Mutoh, T., Tokuda, A., Inokuchi, J., & Kuriyama, M. (1998). Glucosylceramide synthase inhibitor inhibits the action of nerve growth factor in PC12 cells. *Journal of Biological Chemistry*, 273, 26001–26007. https://doi.org/10.1074/jbc.273.40.26001.

Nilsson, O., & Svennerholm, L. (1982). Accumulation of glucosylceramide and glucosylsphingosine (psychosine) in cerebrum and cerebellum in infantile and juvenile Gaucher disease. *Journal of Neurochemistry*, 39, 709–718. https://doi.org/10.1111/j.1471-4159.1982.tb07950.x.

Orvisky, E., Park, J. K., LaMarca, M. E., Ginns, E. I., Martin, B. M., Tayebi, N., & Sidransky, E. (2002). Glucosylsphingosine accumulation in tissues from patients with Gaucher disease: correlation with phenotype and genotype. *Molecular Genetics and Metabolism*, 76, 262–270. https://doi.org/10.1016/S1096-7192(02)00117-8.

Polo, G., Burlina, A. P., Kolamunnage, T. B., Zampieri, M., Dionisi-Vici, C., Strisciuglio, P., Zaninotto, M., Plebani, M., & Burlina, A. B. (2017). Diagnosis of sphingolipidoses: A new simultaneous measurement of lysosphingolipids by LC-MS/MS. *Clinical Chemistry and Laboratory Medicine*, 55, 403–414.

Revel-Vilk, S., Fuller, M., & Zimran, A. (2020). value of Glucosylsphingosine (Lyso-Gb1) as a biomarker in Gaucher disease: A systematic literature review. *International Journal of Molecular Sciences*, 21, 7159. https://doi.org/10.3390/ijms21197159.

Richards, S., Larson, C. J., Koltun, E. S., Hanel, A., Chan, V., Nachtigall, J., Harrison, A., Aay, N., Du, H., Arcalas, A., Galan, A., Zhang, J., Zhang, W., Won, K. A., Tam, D., Qian, F., Wang, T., Finn, P., Ogilvie, K., … Kearney, P. (2012). Discovery and characterization of an inhibitor of glucosylceramide synthase. *Journal of Medicinal Chemistry*, 55, 4322–4335. https://doi.org/10.1021/jm300122u.

Rolfs, A., Giese, A. K., Grittner, U., Mascher, D., Elstein, D., Zimran, A., Böttcher, T., Lukas, J., Hübner, R., Gölnitz, U., Röhle, A., Dudesek, A., Meyer, W., Wittstock, M., & Mascher, H. (2013). Glucosylsphingosine is a highly sensitive and specific biomarker for primary diagnostic and follow-up monitoring in Gaucher disease in a non-Jewish, Caucasian cohort of Gaucher disease patients. *PLoS One*, 8, e79732. https://doi.org/10.1371/journal.pone.0079732.

Sardi, S. P., Viel, C., Clarke, J., Treleaven, C. M., Richards, A. M., Park, H., Olszewski, M. A., Dodge, J. C., Marshall, J., Makino, E., Wang, B., Sidman, R. L., Cheng, S. H., & Shihabuddin, L. S. (2017). Glucosylceramide synthase inhibition alleviates aberrations in synucleinopathy models. *Proceedings of the National Academy of Sciences of the United States of America*, 114, 2699–2704. https://doi.org/10.1073/pnas.1616152114.

Sato, S., Tohyama, K., & Kosugi, Y. (2020). Investigation of MDR1-overexpressing cell lines to derive a quantitative prediction approach for brain disposition using in vitro efflux activities. *European Journal of Pharmaceutical Sciences*, 142, 105119.

Schiffmann, R., Fitzgibbon, E. J., Harris, C., DeVile, C., Davies, E. H., Abel, L., van Schaik, I. N., Benko, W., Timmons, M., Ries, M., & Vellodi, A. (2008). Randomized, controlled trial of miglustat in Gaucher's disease type 3. *Annals of Neurology*, 64, 514–522.

Schueler, U. H., Kolter, T., Kaneski, C. R., Blusztajn, J. K., Herkenham, M., Sandhoff, K., & Brady, R. O. (2003). Toxicity of glucosylsphingosine (glucopsychosine) to cultured neuronal cells: a model system for assessing neuronal damage in Gaucher disease type 2 and 3. *Neurobiology of Diseases*, 14, 595–601.

Shayman, J. A. (2010). Eliglustat tartrate: glucosylceramide synthase inhibitor treatment of type 1 gaucher disease. *Drugs Future*, 35, 613–620. https://doi.org/10.1358/dof.2010.035.08.1505566.

Skotland, T., Ekroos, K., Kavaliauskiene, S., Bergan, J., Kauhanen, D., Lintonen, T., & Sandvig, K. (2016). Determining the turnover of glycosphingolipid species by stable-isotope tracer lipidomics. *Journal of Molecular Biology*, 428, 4856–4866.

Smid, B. E., Ferraz, M. J., Verhoek, M., Mirzaian, M., Wisse, P., Overkleeft, H. S., Hollak, C. E., & Aerts, J. M. (2016). Biochemical response to substrate reduction therapy versus enzyme replacement therapy in Gaucher disease type 1 patients. *Orphanet Journal of Rare Diseases*, 11, 28.

Smid, B. E., & Hollak, C. E. M. (2014). A systematic review on effectiveness and safety of eliglustat for type 1 Gaucher disease. *Expert Opinion on Orphan Drugs*, 2, 523–529.

Sueyoshi, N., Maehara, T., & Ito, M. (2001). Apoptosis of Neuro2a cells induced by lysosphingolipids with naturally occurring stereochemical configurations. *Journal of Lipid Research*, 42, 1197–1202. https://doi.org/10.1016/S0022-2275(20)31569-8.

Treiber, A., Morand, O., & Clozel, M. (2007). The pharmacokinetics and tissue distribution of the glucosylceramide synthase inhibitor miglustat in the rat. *Xenobiotica*, 37, 298–314. https://doi.org/10.1080/00498250601094543.

van Eijk, M., Ferraz, M. J., Boot, R. G., & Aerts, J. M. F. G. (2020). Lyso-glycosphingolipids: Presence and consequences. *Essays in Biochemistry*, 64, 565–578. https://doi.org/10.1042/EBC20190090.

Weiss, K., Gonzalez, A., Lopez, G., Pedoeim, L., Groden, C., & Sidransky, E. (2015). The clinical management of type 2 Gaucher disease. *Molecular Genetics and Metabolism*, 114, 110–122.

Wennekes, T., Meijer, A. J., Groen, A. K., Boot, R. G., Groener, J. E., van Eijk, M., Ottenhoff, R., Bijl, N., Ghauharali, K., Song, H., O'Shea, T. J., Liu, H., Yew, N., Copeland, D., van den Berg, R. J., van der Marel, G. A., Overkleeft, H. S., & Aerts, J. M. (2010). Dual-action lipophilic iminosugar improves glycemic control in obese rodents by reduction of visceral glycosphingolipids and buffering of carbohydrate assimilation. *Journal of Medicinal Chemistry*, 53, 689–698.

Xu, Y. H., Quinn, B., Witte, D., & Grabowski, G. A. (2003). Viable mouse models of acid beta-glucosidase deficiency: The defect in Gaucher disease. *American Journal of Pathology*, 163, 2093–2101.

SUPPORTING INFORMATION

Additional supporting information may be found online in the Supporting Information section.

How to cite this article: Fujii, T., Tanaka, Y., Oki, H., Sato, S., Shibata, S., Maru, T., Tanaka, Y., Tanaka, M., & Onishi, T. (2021). A new brain-penetrant glucosylceramide synthase inhibitor as potential Therapeutics for Gaucher disease. *Journal of Neurochemistry*, 159, 543–553. https://doi.org/10.1111/jnc.15492